IEEE Access
Multidisciplinary ⋮ Rapid Review ⋮ Open Access Journal

Received November 30, 2021, accepted December 16, 2021, date of publication January 7, 2022, date of current version January 13, 2022.

Digital Object Identifier 10.1109/ACCESS.2022.3141588

A Project-Based Learning Approach for Building an Affordable Control Teaching Lab: The Centrifugal Ring Positioner

XAVIER JORDENS, ROBIN WILMART, EMANUELE GARONE, (Member, IEEE), MICHEL KINNAERT, (Member, IEEE), AND LAURENT CATOIRE
Department of Control Engineering and System Analysis, Université Libre de Bruxelles, 1050 Bruxelles, Belgium
Corresponding author: Xavier Jordens (xavier.jordens@ulb.be)

ABSTRACT This paper presents a novel experimental setup for teaching control engineering. This setup was developed during a project-based learning activity. The approach consists in training a master student in mechatronics and control through the design, manufacturing, and control of a device that will contribute over time to the education of students by laboratory sessions based on the device. The latter is an easy-to-build, reproducible, and affordable experimental setup called the Centrifugal Ring Positioner (CRP). It aims at illustrating several concepts of closed-loop control (e.g. system identification, model validation, and controller design and validation) while getting acquainted with typical experimental issues like the handling of measurement noise and the real-time implementation of a control law. The CRP distinguishes itself from most pedagogical benchmarks by the wide use of 3D printing. It is an unstable and nonlinear system, consisting of a ring able to slide on a rod thanks to the balance between gravity and centrifugal force. The control of the system aims at stabilizing the ring at any fixed position on the rod. The complete methodology followed during the project-based learning approach to build and control a CRP is detailed, including derivation of a dynamic model based on classical mechanics theory, considerations on the mechanical design, selection of the components, step response and physics-based model identification, and PID controllers design based on computer-assisted methods such as root locus and Bode diagrams.

INDEX TERMS 3D printing, centrifugal ring positioner, control engineering education, control systems, mechatronics, teaching lab.

I. INTRODUCTION

Control systems are present in many fields in today's world, ranging from manufacturing processes to consumer products. Implementation of new technological systems is partially possible thanks to the evolution of control theory; this evolution being closely linked to teaching activities and constantly evolving research. Control engineering students should be able to make connections between theoretical and practical control systems concepts (data acquisition system, real-time software, sensors…) through practical experiments [1], [2]. They must have the opportunity to confront the theory to practical cases to become aware of potential imperfections arising from real systems complexity such as disturbances, measurement noises, and model uncertainties [3]. Hands-on experimentations should allow to verify classical techniques, perform model validation experiments, and develop new tools and verify their implementation [1], [4]. This reflection is what is stimulating within research and teaching the idea of developing pedagogical benchmark systems. Such benchmarks should illustrate control theory aspects such as stabilization of open-loop unstable systems, setpoint tracking, and disturbance rejection [5]. Requested characteristics for these systems are: good illustration of theoretical concepts, good visualization of the physics of the device, low-cost assembly, repeatability, reliability, and easy use and understanding [6]. Among the best-known control laboratory systems are the inverted pendulum and the ball and beam [4].

However, due to the growing interest in control engineering, the number of students enrolled in control courses increases each year. This implies a higher financial need for laboratory equipment (need of more pedagogical

The associate editor coordinating the review of this manuscript and approving it for publication was Bidyadhar Subudhi.

benchmarks, space, and maintenance) and the need for more teaching staff [7]. As this can not always be easily implemented, students end up with limited access to the lab and hence a lower number of practical activities [8], [9]. Remote laboratories (RLs) have been imagined to overcome this problem. They are usually proposed as a complement to traditional labs and consist of real plants or devices that are operated remotely through an Internet connection via a user-friendly interface [10], [11]. RLs allow increasing the time for the students to perform experiments since they can practice whenever they have internet access. Moreover, these labs do not need the same amount of supervision as usual labs, hence freeing up time for the teaching staff [12]. However, like all control systems benchmarks, RLs usually need important investment in terms of equipment, space, and maintenance. It is noteworthy to mention also that they can not completely replace traditional in-the-presence labs since they do not provide the same experience as performing face-to-face experiments, which could, in addition, lead to a loss of attractivity for the students [9], [13].

In addition to RLs, Virtual Labs (VLs) have also emerged. Those consist of computer-based simulations of real plants. The main advantages of VLs are their low cost and their very limited need for physical material and maintenance. They thus allow students to perform experiments on many simulated plants of any kind of complexity. Besides, they offer the possibility of easily changing parameters to analyze their respective influence on the plant [10], [11]. VLs however present as the main drawback the fact of being less attractive for the students. Moreover, developing VLs from scratch could sometimes require a huge effort [14].

To go a step further in control education, the current emergence of Take-Home Labs (THLs) must be discussed. THLs consist of compact, low-cost (usually less than 200€), and easy-to-assemble kits that allow students to perform experiments at home with the computational power provided by their computer [3], [15]. Example of take-home lab experiments are LED brightness control [15], temperature control [13], [15], DC motor control [13], [15], and analog filter system [7]. The main challenge of THLs design is to build cheap but robust and easy-to-use devices that are still able to produce a sufficient range of experiments with coherent results [7], [13]. Indeed this kind of lab is usually used for basic control courses. Hence, the different devices should exhibit similar and reproducible behaviors that can be modeled accurately by a low-order dynamic model. Ensuring and illustrating the coherence between the experimental results and the estimated mathematical models is indeed essential for a proper understanding of the course material. THLs present advantages compared to RLs and VLs in that students can perform experiments on their own, increasing their interest and their involvement. They have more freedom and can work at their own rhythm [3], [7]. Some observations are however in order. On the one hand, THLs make the students more invested, which is positive for the mastery of a specific course. On the other hand, this investment must be accounted for by a proper accounting of the work done at home in the students' load. Otherwise, students would be overwhelmed by the extra work required by each course. Besides, it is noteworthy that THLs might require a major, and sometimes unrealistic, involvement of the teaching staff. Numerous guidance sessions must be implemented to support students during their work and large maintenance is expected since students transport setups and perform experiments without direct monitoring.

Finally, it should be mentioned that, in parallel to THLs, most experimental setups are developed using low-cost microcontrollers such as Arduino, Raspberry Pi, or similar. For example, in [16], a low-cost quadcopter is developed using an Arduino-based platform with cheap compatible sensors, that allows training students in system modeling, identification, and PID control. Reference [17] presents a simplified helicopter test-bench using a Raspberry Pi to train students in controller design. More and more two-wheels self-balancing robots are also reported in the literature [18]–[20]. Those are currently mainly used as on-site laboratory devices but could be used as take-home devices. Along the same lines, [21] presents an Arduino-based thermal regulation kit to teach modeling and control concepts. The kit is meant to be used during laboratory sessions but could be requested by the students for performing home experiments. Such low-cost experimental setups constitute a good inspiration for the future of take-home education. However, some of these attractive setups are mobile and hence need a battery. Therefore, the use of such setups for laboratory sessions adds a constraint for the teaching staff, namely dealing with the charging of the batteries. In addition, applications such as yaw control of helicopters, or tilt angle control of self-balancing robots require precise yaw or tilt measurement that is usually achieved with an IMU. Such sensor could require instrumentation concepts out of the scope of control courses such as data fusion and are therefore usually given as a black box to the students. The same goes for the modeling of some setups such as propeller devices, that could require complex mechanical concepts.

The objective of this paper is to present a novel on-site benchmark for teaching control engineering courses presenting an interesting compromise among already well-known benchmarks, RLs, VLs, and THLs, as discussed below. This device is called the Centrifugal Ring Positioner (CRP). The CRP was developed within a project-based learning activity set up for several years in our control department. This approach lies in assigning to a student a project, usually for his master thesis, consisting in creating a pedagogical device that will be used afterward by control engineering students. The interest of this approach is to train a student in mechatronics and control through the creation of the device in a first stage, and to contribute to the education of other students by laboratory sessions based on this device in a second phase. This approach has already led to the

development of several experimental setups such as a ball in the tube, a cart inverted pendulum, and a rotary inverted pendulum.

In terms of learning content, the CRP is an unstable and nonlinear system, that allows to illustrate several control systems concepts (system identification, model validation, PID control, state-feedback control, LQG control…) with a significant multidisciplinary aspect (instrumentation, signal processing, classical mechanics…). Compared to existing pedagogical benchmarks such as the inverted pendulum or the ball and beam, the CRP presents the advantage of being mostly 3D-printed (using Poly-Lactic Acid (PLA) as material). This offers a large amount of freedom in its design coupled with a relatively low cost (<1000€). Besides, it results in a quite easily reproducible device. Based on its components, it is expected that the CRP requires very limited maintenance over time. This combined with its low price, its reproducibility, and its compact design allows to use simultaneously a high number of devices without needing a lot of space. Hence more students could perform experiments at the same time and thereby increase their lab time. In its current version, the CRP is less compact than typical THLs but it has the advantage of providing a strong visual illustration of control concepts through the ring motion. This visual feature is often set aside in THLs (e.g. temperature control). Yet it should not be disregarded as it strongly increases the curiosity and the interest of the students. Compared to most low-cost microcontroller-based setups, the CRP is completely transparent for the students. In terms of instrumentation, the two sensors (namely the infrared distance sensor and the rotary encoder) are easy-to-use and allow the students to directly work with their output signals. Furthermore, the modeling can be completely achieved with classical concepts of mechanics. Finally, the CRP is a fixed setup and hence does not require a battery.

This paper focuses on the design process, the selection of the components for the CRP, and the control of the built devices. It emphasizes the multidisciplinary nature of project-based learning on which the design of the device is based by exhibiting the strong interconnections between mechanical design, proper choice of sensors and actuators, and control performance. A repository with the teaching material, the plans of the different parts, the specifications of the actuators and sensors as well as the control codes so that the device can be reproduced can be found on the following website: https://github.com/Xavier-Jds/Centrifugal-Ring-Positioner. All the construction plans and the software are released under license CC BY-NC-SA 4.0 (for the purpose of this license academic and training usage are to be considered non-commercial).

The paper is organized as follows: Section II describes the design process of the CRP and presents the derivation of its dynamic model. Then, Section III tackles the control of the CRP, and Section IV discusses the key teaching aspects of the device. Finally, Section V presents conclusions and potential future work.

II. DESCRIPTION OF THE CRP

A. DEVICE AND COMPONENTS

1) DEVICE

The CRP (Fig. 1) is a nonlinear unstable mechanical system consisting of a mobile hollow cylinder, the so-called ring, able to slide on a tilted rod (3 and 8, respectively, in Fig. 1). The rod is coupled to the shaft of a motor (3, in Fig. 1) allowing its rotation around the vertical axis.

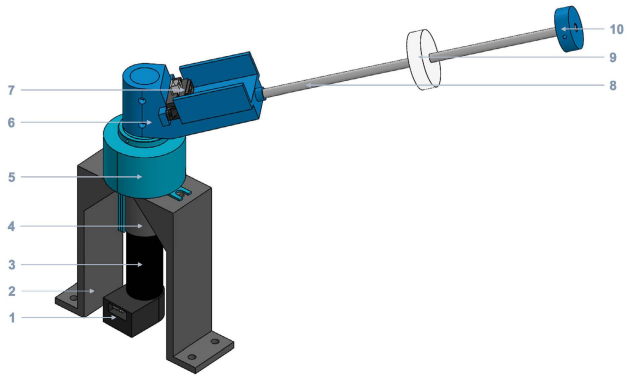

FIGURE 1. 3D representation of the CRP (1: encoder, 2: motor support, 3: motor, 4: reduction gear, 5: slip ring, 6: coupling pieces, 7: position sensor, 8: rod, 9: ring, 10: ring stop).

The ring motion is driven by gravity and centrifugal force. Equilibrium points correspond to ring positions on the rod where these two forces are balanced. The equilibria of the system are unstable since a small variation in the equilibrium angular velocity induces the motion of the ring towards one rod end. The objective of the control of the CRP consists in the tracking of the ring position by acting on the system input, namely the motor current.

2) OVERALL DESIGN

The design of the CRP has been thought to emphasize the visual aspect of the control of the system while keeping a low-cost and easy-to-build device. A preliminary idea was to consider a ball inside a tube, similar to the ball in the tube benchmark [22]. This would however have strongly constrained the choice of material and geometry of the arm. The configuration of a ring sliding on a rod appeared to be the more practical to implement, still allowing a good visual representation of the ring position and motion. Except for the rod, all the mechanical pieces of the CRP have been 3D-printed using Poly-Lactic Acid (PLA) filaments. 3D printing offers many advantages such as low price, high freedom in the design, low weight of the final device, and the opportunity of creating complex pieces. The following sections detail the different pieces constituting the CRP and the considerations that guided their selection and design.

3) ACTUATOR

The actuator of the CRP consists of a motor and the associated equipment (motor driver, power supply, and encoder). The

main requirement for the actuator is to be able to provide a sufficiently large torque at any moment. Besides, the velocities required for the control must not exceed the nominal velocity of the motor. As will be detailed in Section II-B by (8), the equilibrium points of the CRP are directly related to the rod tilt angle. This angle also influences the torques that the actuator should be able to provide. The rod tilt angle has been chosen to be 20° (see Section II-A9). The selection of the actuator has been performed in the following way:

- To have a preliminary indication of the range of velocities of the motor, equilibrium velocities for a tilt angle of 20° have been calculated considering ring positions between 0.03 m and 0.28 m (Fig. 2). From this analysis it resulted that the nominal velocity of the motor must be higher than 107 rpm if the minimal ring position on the rod is 0.03 m.

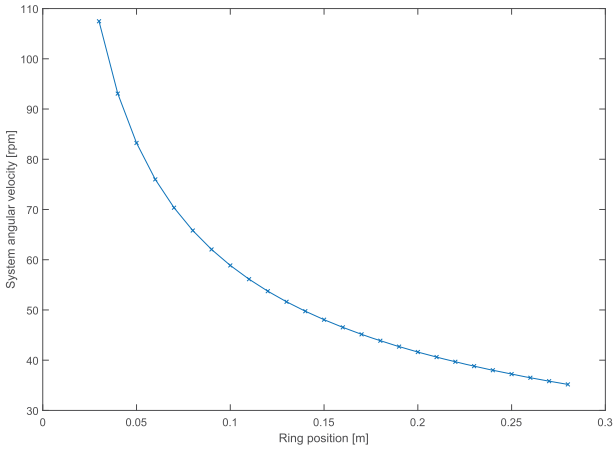

FIGURE 2. Equilibrium ring positions and corresponding angular velocities of the CRP for a tilt angle of 20°.

- Thereafter, simulations of the CRP with a tilt angle of 20° have been performed to get an idea of the range of the torques that the actuator should provide. These simulations were based on the system dynamics that will be detailed in Section II-B. Tentative values of system parameters required for the simulations were selected based on a preliminary design of the device. A preliminary PID controller has been designed to control the ring position via a cascade control. Fig. 3 depicts an extreme case of the control, consisting in bringing the ring from a high position of 0.28 m to a low position of 0.03 m. Among all the transitions between two different ring positions, this represents the situation where the required torque has the highest value. A ramp reference is used for smoother ring transitions. Simulations show that the torque never exceeds 0.7 Nm. In addition, a safety margin of 100% was considered for taking into account unquantified parameters such as friction and potential changes of system parameters.

Based on this discussion, a Maxon DC gearmotor RE25 Precious Metal Brushes CLL 10W with encoder HEDS 5540

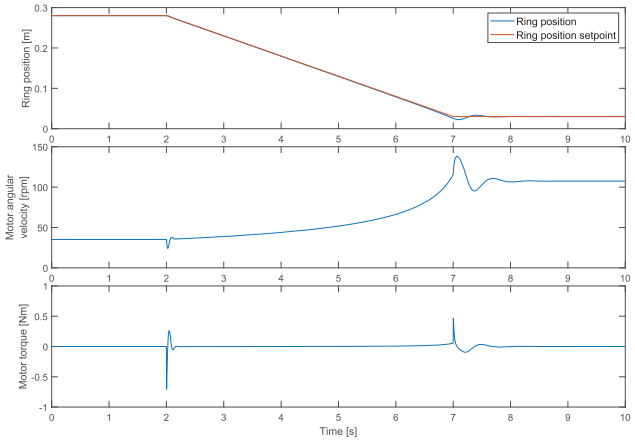

FIGURE 3. Preliminary control simulation of the CRP for a tilt angle of 20°. The ring is moved from an equilibrium position of 0.28 m to an equilibrium position of 0.03 m.

(3 and 1, respectively, in Fig. 1) coupled to an Escon 50/5 motor driver (fed by a 24V power supply) has been selected. Indeed, the nominal velocity of this motor is about 118 rpm and it can provide a maximal torque of 4 Nm (which exceeds our requirements). Note that in Fig. 3, the motor angular velocity exceeds the nominal velocity of the motor at about 7 s. Please remind this simulation represents an extreme case and this velocity is required only for a very short time.

4) SENSORS

For the ring position, contactless sensors such as infrared or ultrasonic sensors were investigated since they induce fewer constraints on the system design if compared to contact sensors such as potentiometers. Among potential candidates, the Sharp GP2Y0A41SK0F infrared position sensor (7, in Fig. 1) was selected for its short measuring cycle and its measuring range completely compatible with the rod length. Since the part of the system containing the microcontroller is stationary and the part containing the sensor is rotating, a slip ring (5, in Fig. 1) is needed to make the electrical connections between both parts. The encoder already coupled to the selected motor is used for estimating the angular velocity of the system, on the basis of the measured motor angular position.

5) CONTROLLER DEVICE

An Arduino DUE microcontroller, programmed via the Arduino IDE, has been chosen as controller device for its portability and its high computing power.

6) MOTOR SUPPORT

The encoder below the gearmotor is not intended to support the weight of the overall system. For this reason, a motor support (2, in Fig. 1) was designed to make the connection between the system and a wooden board serving as a base. The upper side of the piece contains a large hole in the middle surrounded by four screw holes to carry the gearmotor and

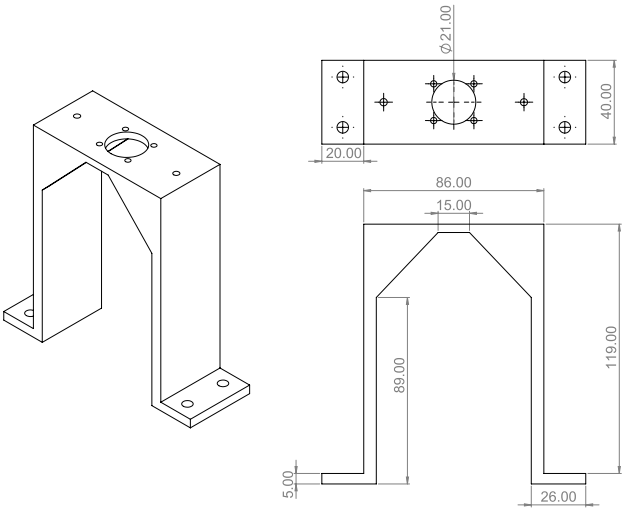

FIGURE 4. Plans of the motor support.

incorporate its shaft (see Fig. 4). This part of the piece also contains two screw holes for fixing the stationary part of the slip ring. On the lower parts, the piece has four screw holes aiming at fixing it to the wooden board. Diagonal reinforcements have been added to increase the mechanical resistance of the support.

7) ROD

The rod is realized in Aluminum. This material was selected for its stiffness and its lightness. It has a circular section of 6 mm diameter and its length has been limited to 176 mm to keep the device compact (the ring can only slide on 126 mm, the 50 mm left are nested inside the coupling piece). A small diameter was chosen to limit the contact area with the ring and hence reduce friction. Selecting a rod with as few imperfections as possible is important to have the most homogeneous ring friction coefficient all along the rod. A 3D-printed stop piece (10, in Fig. 1) is fixed at the end of the rod.

8) RING

Using 3D printing for the ring (9, in Fig. 1) offered the opportunity to test several parameters such as external dimension (to enhance position measurement), inner dimension (to reduce friction), or weight, to reach the best performances. By testing different ring inner diameters, the best sliding conditions on the rod were observed for an inner diameter of 6.3 mm. Besides, to limit external disturbances in the position measurements, the ring diameter must be higher than 40 mm. It has been chosen to be slightly higher, namely 50 mm. The ring thickness has been chosen to be 10 mm to have a fairly high weight and sufficient guidance along the rod.

9) COUPLING PIECES

The two coupling pieces (6, in Fig. 1), namely the motor coupling and the rod coupling, aim at connecting the rod to the shaft of the motor. The motor coupling (Fig. 5) consists

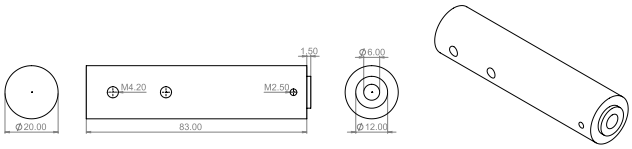

FIGURE 5. Plans of the motor coupling piece.

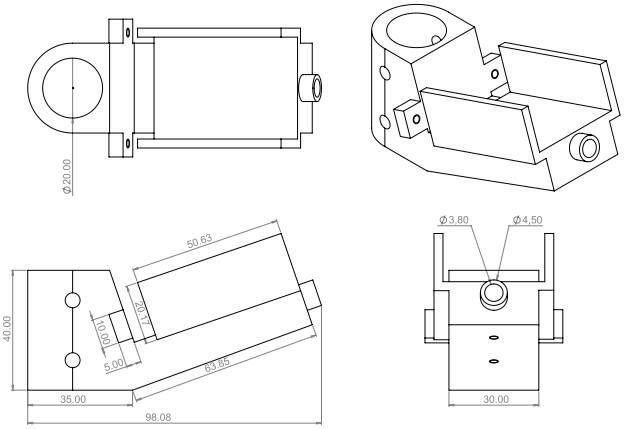

FIGURE 6. Plans of the rod coupling piece.

of a cylinder containing a small hole on its bottom side to nest the motor shaft and fix it with a clamping screw. On its upper part, the motor coupling piece contains two holes to fix the rod coupling piece with screws. The motor coupling is relatively long since there must be enough space between the motor and the rod coupling to place the slip ring.

Regarding the rod coupling piece (Fig. 6), 3D printing allowed again to create the complex shapes required to meet the needs. It is through this piece that the rod angle is defined. The higher the angle, the higher the equilibrium velocities. That can affect the proper visualization of the ring position, which impairs the visual side of the CRP. However, if the angle is too low, the action of the gravity might not be sufficient to overcome the static friction and offer good control performances. A value of 20° turned out to provide an appropriate trade-off between these two needs.

On one side, the piece contains a large cylindrical hole to be nested and fixed around the motor coupling piece. On the other side, it contains a smaller cylindrical hole in which the rod can be inserted and fixed from below with two clamping screws. The distance between the sensor (7, in Fig. 1) and the lowest ring position on the rod was chosen to be higher than the lower limit of the measuring range of the sensor (i.e., higher than 40 mm). A sensor hosting seat and walls have been added on each side of the piece after performing experiments to decrease external measurement disturbances. The experiments consisted in placing rings of different diameters at the same distance of the sensor, and taking a series of measurements for each ring, at first without the seat and the walls, and then with them.

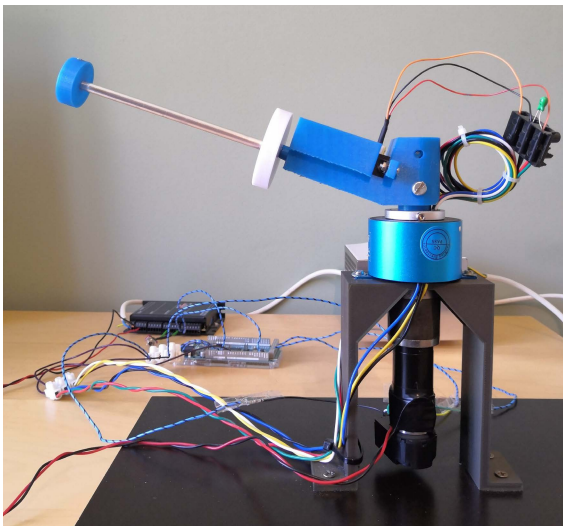

FIGURE 7. Picture of the CRP.

10) FILTERING

The rotation of the slip ring strongly affects the signal of the ring position sensor. This is due to contact failures inside the slip ring, which can lead on the one hand to some losses of sensor energy supply, and on the other hand to some losses of the measurement signal. To stabilize the sensor supply voltage, a 10 μF capacitor has been placed on the supply wire, between the slip ring and the sensor. Regarding the measurement signal, a capacitor was placed on the output voltage of the sensor on the Arduino side, aiming at filtering high signal frequencies. After comparing several capacitors, a trade-off value of 330 nF was selected which ensures a smooth but not significantly phase-shifted signal.

11) FINAL DEVICE

Fig. 7 shows the CRP built by assembling the elements described in the previous subsections.

B. DYNAMIC MODEL OF THE CRP

The dynamic model of the CRP can be derived using relatively simple concepts of classical mechanics. Table 1 contains the parameters that are involved in the mathematical development. The following Table will serve as reference for all the parameters mentioned further on in this section.

TABLE 1. List of the parameters involved in the mathematical development of the dynamic model of the CRP.

Symbol	Quantity	Units
m	mass of the ring	kg
ω	CRP angular velocity	rad/s
θ	tilt angle of the rod	$^\circ$
g	acceleration of gravity	m/s^2
p	ring position on the rod	m
r	distance of the ring with the rotational axis	m
c	ring viscous friction coefficient	kg/s
i	motor current	A
K	motor torque constant	Nm/A
f	motor viscous friction coefficient	Nm/s
C_r	motor resistive torque	Nm

Fig. 8a and 8b are simplified representations of the CRP to illustrate the derivation of its dynamic model.

Applying the second Newton's law of motion along the rod axis, namely $\vec{1}_t$, yields

$$\sum \vec{F} = m\vec{a}_r + m\vec{a}_c + m\vec{a}_{cor}, \tag{1}$$

where $\sum \vec{F}$ is the sum of the forces applied on the ring, and $\vec{a}_r$, $\vec{a}_c$, and $\vec{a}_{cor}$ are the relative, the centripetal, and the Coriolis acceleration of the ring, respectively.

Replacing each term with its mathematical expression gives the following relation between the ring motion and the rotational velocity of the system:

$$-mgsin\theta - c\dot{p} = m\ddot{p} - mp\omega^2 cos^2\theta. \tag{2}$$

To obtain a state-space representation, a second equation including the system input (i.e., the motor current) must be found. This can be obtained by applying the angular momentum theorem in O (defined as the intersection of the rod with the vertical motor shaft, see Fig. 8) along the $\vec{1}_Z$ axis, i.e.

$$\frac{d\vec{M}_{O,Z}}{dt} = \vec{m}_{e,O,Z}, \tag{3}$$

where $\vec{M}_{O,Z}$ is the Z-component of the angular momentum of the CRP calculated in O and $\vec{m}_{e,O,Z}$ is the Z-component of the external momentum applied in O.

Replacing each term by its expression leads to

$$i_{33}\dot{\omega} + mp^2 cos^2\theta\dot{\omega} + 2mp\dot{p}\omega cos^2\theta = Ki - C_r - f\omega, \tag{4}$$

where i_{33} represents the element $_{3,3}$ of the inertia tensor of the CRP.

The nonlinear dynamics of the CRP is obtained by combining (2) and (4), and performing some mathematical manipulations:

$$\begin{cases} \ddot{p} = -gsin\theta - \frac{c}{m}\dot{p} + p\,\omega^2 cos^2\theta \\ \dot{\omega} = \dfrac{(Ki - C_r - f\omega - 2mp\dot{p}\omega cos^2\theta)}{(i_{33} + mp^2 cos^2\theta)}. \end{cases} \tag{5}$$

Model (5) can be rewritten in state-space form $\dot{x} = \phi(x, u)$ by introducing the following state vector x and state input u:

$$x = \begin{bmatrix} x_1 \\ x_2 \\ x_3 \end{bmatrix} = \begin{bmatrix} p \\ \dot{p} \\ \omega \end{bmatrix}, \quad u = \begin{bmatrix} i \end{bmatrix}, \tag{6}$$

leading to:

$$\begin{cases} \dot{x}_1 = x_2 \\ \dot{x}_2 = -gsin\theta - \dfrac{c}{m}x_2 + x_1\, x_3^2 cos^2\theta \\ \dot{x}_3 = \dfrac{(Ku - C_r - fx_3 - 2mx_1x_2x_3cos^2\theta)}{(i_{33} + mx_1^2 cos^2\theta)}. \end{cases} \tag{7}$$

To the equilibrium input $\bar{u}$ corresponds the equilibrium point

$$\bar{x} = \begin{bmatrix} \bar{x}_1 \\ \bar{x}_2 \\ \bar{x}_3 \end{bmatrix} = \begin{bmatrix} \dfrac{gsin\theta}{\bar{x}_3^2 cos^2\theta} \\ 0 \\ \dfrac{K\bar{u} - C_r}{f} \end{bmatrix}. \tag{8}$$

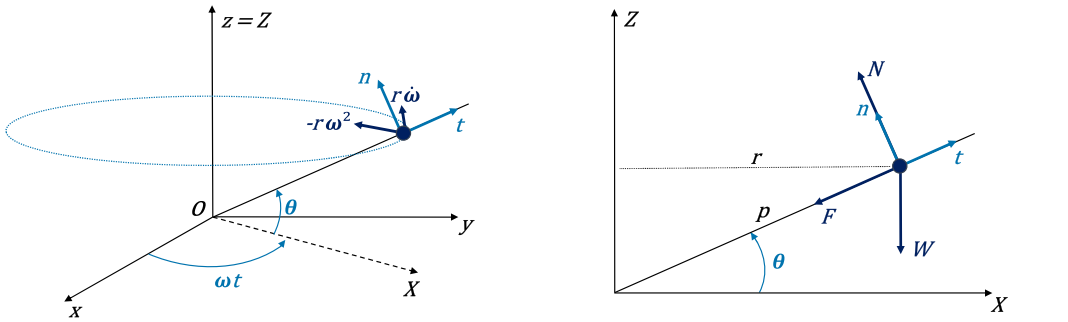

(a) 3D representation.

(b) 2D representation (N = normal, F = friction and W = weight).

FIGURE 8. Simplified representations of the CRP.

Considering small deviations $\tilde{x}$ around an equilibrium point, model (7) can be linearized:

$$\dot{\tilde{x}} = \left[\frac{\delta\phi}{\delta x}\right]_{\substack{x=\bar{x}\\u=\bar{u}}} \tilde{x} + \left[\frac{\delta\phi}{\delta u}\right]_{\substack{x=\bar{x}\\u=\bar{u}}} \tilde{u}, \tag{9}$$

where $\frac{\delta\phi}{\delta x}$ is the Jacobian of ϕ with respect to x and $\frac{\delta\phi}{\delta u}$ is the Jacobian of ϕ with respect to u.

Since two measurements are available on the CRP, namely the ring position and the motor angular velocity (the angular velocity is here assumed to be measured, knowing that it is estimated from the motor encoder), $\tilde{x}_1$ and $\tilde{x}_3$ are chosen as outputs. This yields to the linearized state-space representation

$$\begin{bmatrix}\dot{\tilde{x}}_1\\ \dot{\tilde{x}}_2\\ \dot{\tilde{x}}_3\end{bmatrix} = \begin{bmatrix} 0 & 1 & 0 \\ \bar{x}_3^2 cos^2\theta & -\frac{c}{m} & 2\bar{x}_1\bar{x}_3 cos^2\theta \\ 0 & -\frac{2m\bar{x}_1\bar{x}_3 cos^2\theta}{i_{33}+m\bar{x}_1^2 cos^2\theta} & -\frac{f}{i_{33}+m\bar{x}_1^2 cos^2\theta}\end{bmatrix} \cdot \begin{bmatrix}\tilde{x}_1\\ \tilde{x}_2\\ \tilde{x}_3\end{bmatrix} + \begin{bmatrix} 0 \\ 0 \\ \frac{K}{i_{33}+m\bar{x}_1^2 cos^2\theta}\end{bmatrix}\tilde{u}$$

$$\begin{bmatrix}\tilde{y}_1\\ \tilde{y}_2\end{bmatrix} = \begin{bmatrix}1 & 0 & 0\\ 0 & 0 & 1\end{bmatrix}\begin{bmatrix}\tilde{x}_1\\ \tilde{x}_2\\ \tilde{x}_3\end{bmatrix} + \begin{bmatrix}0\\ 0\end{bmatrix}\tilde{u}. \tag{10}$$

III. CONTROL OF THE CRP

The CRP will be used for lab sessions aiming at designing and implementing a control strategy that meets one or several requirements for a real plant. The requirement of the CRP consists in stabilizing the ring at any fixed position on the rod with no steady-state error. Besides this, students are asked to design their controllers in such a way that a reasonable trade-off is achieved between robustness (e.g., in terms of phase and gain margins), overshoot, and tracking performances. In this section, an example of the work expected from students is outlined.

A. CONTROL STRATEGY

The selection of the control strategy starts by analyzing the system and the requirements. The aim is to control the position of the ring according to a setpoint by acting on the only system input, i.e., the motor input current. Equation (2) and its linearization show that the ring position is directly linked to the system angular velocity. Moreover, for the selected gearmotor, a small input current change results in an important velocity variation, and the current-velocity relation is not linear (friction, saturation). Introducing a cascade control scheme [23], [24] (Fig. 9) with an inner loop controlling the motor angular velocity allows to design a simple and efficient controller for the ring position. This can be implemented since the angular velocity of the motor can be numerically estimated from the encoder measurements.

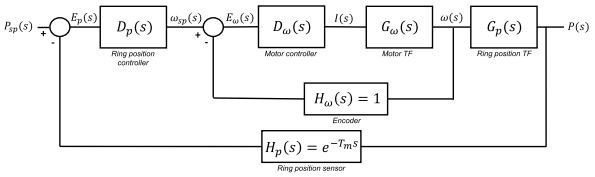

FIGURE 9. Cascade control block diagram of the CRP. Transfer functions (TF) of the sensors are assumed to have an unitary gain. The ring position sensor TF accounts for the short measuring cycle of the selected sensor.

B. MODELS IDENTIFICATION

Designing the controllers for the cascade scheme using basic design methods requires a transfer function for each of the subsystems ($G_\omega(s)$ and $G_p(s)$). Theoretically, the state-space representation (10) allows obtaining both transfer functions via a white-box approach. The ring position transfer function (11) is obtained using the parameters of Table 2. The minimal ring position on the rod (i.e., 0.08 m) is chosen as the equilibrium position since it corresponds to the natural initial position of the ring. The ring viscous friction coefficient has been determined by parameters identification from a data set

TABLE 2. Parameters involved in the ring position transfer function (11).

Symbol	Quantity	Value
ring mass	m	$0.0239\ kg$
equilibrium ring position	$\bar{p}$	$0.08\ m$
equilibrium CRP angular velocity	$\bar{\omega}$	$6.89\ rad/s$
rod tilt angle	θ	$20°$
ring viscous friction coefficient	c	$0.3\ kg/s$

corresponding to a step-like input current change.

$$rClG_p(s) = \frac{P(s)}{\omega(s)} = \frac{2\bar{p}\bar{\omega}\cos^2\theta}{s^2 + \frac{c}{m}s - \bar{\omega}^2\cos^2\theta} = \frac{0.97}{s^2 + 12.55s - 41.94} \tag{11}$$

For the motor, parameters such as C_r or f involved in its dynamic model are not trivial to quantify. Hence, the motor transfer function is obtained by fitting a black box model to the system response (Fig. 10). First, the motor operating around an equilibrium velocity is subject to an input current step change and data are collected at a sampling time of 1 ms. Then, a first-order model is estimated from the experimental data using least mean squares. This leads to the following model for the motor:

$$G_\omega(s) = \frac{\omega(s)}{I(s)} = \frac{769.44}{1.31s + 1} \tag{12}$$

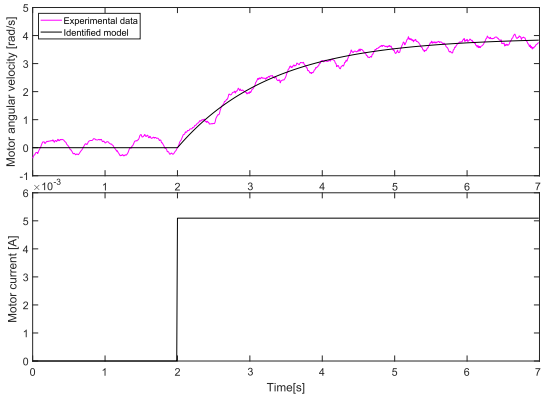

FIGURE 10. Identification of the motor transfer function. The depicted data correspond to variations around the equilibrium velocity and corresponding motor current.

C. DESIGN AND IMPLEMENTATION OF THE CONTROLLERS

Continuous-time controllers are designed for each loop. Next, they are approximated by digital controllers. The continuous-time controller is first designed using the root locus method. A dead time corresponding to one sampling period is taken into account in the loop via Bode diagrams. Such a dead time is considered to approximate the delay effects of the Digital-to-Analog (DAC) and Analog-to-Digital (ADC) converters, and the computation time. A small sampling period must be chosen so that the discrete-time compensator approximates as well as possible the continuous-time controller. The sampling period T_s has been chosen to be 1 ms.

The inner loop controller aims at ensuring the motor response to disturbances before they affect the ring position. Since the transfer function of the motor has been identified as a first-order transfer function, it can be controlled with a simple P controller. The controller is designed considering the speed of response, the saturation of the actuator, and the stability margins. The gain (13) leads to fast responses to sudden velocity setpoint changes without saturating the motor current,

$$D_\omega(s) = k_p = 0.15. \tag{13}$$

Accounting for the inner loop, the system to be controlled by the outer loop controller has the following transfer function:

$$\frac{P(s)}{\omega_{sp}(s)} = \frac{k_p G_\omega(s)}{1 + k_p G_\omega(s)} \times \frac{2\bar{p}\bar{\omega}\cos^2\theta}{s^2 + \frac{c}{m}s - \bar{\omega}^2\cos^2\theta}. \tag{14}$$

The outer loop controller aims at reaching the control requirement, i.e., ring position setpoint tracking. An integrating action is required to cancel any steady-state error during constant setpoint phases. Root loci show that a PI controller is not sufficient to stabilize the outer loop; hence, a PID controller is implemented in the form

$$D_p(s) = k\frac{(1 + sT_i)}{sT_i}\frac{(1 + sT_d)}{(1 + sT_f)}, \tag{15}$$

with $T_f = T_d/N$.

Such a controller presents four parameters that can be tuned to reach the desired closed-loop performance. T_d is chosen so that the corresponding controller zero cancels the negative pole of the system which is closest to the imaginary axis. The filtering time constant T_f is usually chosen to be 8 to 20 times faster than T_d. Despite the measures discussed in Section II-A10, the position sensor signal is still noisy and a sufficiently low value of N ($N = 8$) is therefore required to enhance the filtering action. T_i is selected accounting for its influence on the system stability margins. The gain k is chosen based on the root locus (Fig. 11) so that the complex conjugate poles of the closed-loop response have a damping ratio of 0.7. Such a damping ratio is chosen since it allows a fast response while keeping a limited overshoot. Among the two gains that lead to such a damping ratio, the smallest has been chosen to have to highest stability margins. This leads to the controller transfer function

$$D_p(s) = 285\frac{(1 + 0.150s)}{0.150s}\frac{(1 + 0.065s)}{(1 + 0.008s)}. \tag{16}$$

Accounting for the sampling time of 1 ms and for the dead time of 16.5 ms of the sensor, the stability margins of the CRP coupled with this controller are 7.06 dB and 23°. The low value of phase margin is mainly due to the important dead time introduced in the loop by the position sensor. To implement this controller, the continuous-time control law is approximated into a discrete one using the Tustin method ($T_s = 1$ ms):

$$D_p(z) = \frac{2172z^2 - 4297z + 2125}{z^2 - 1.8850z + 0.8847}. \tag{17}$$

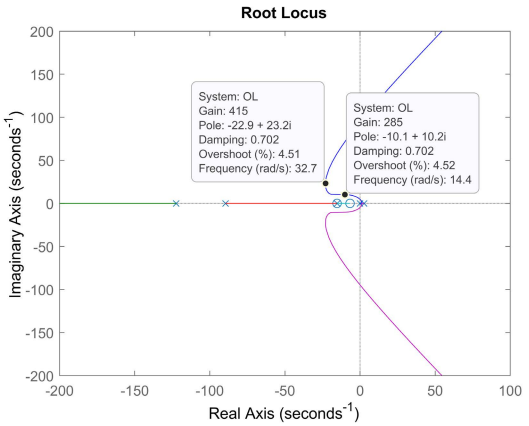

FIGURE 11. Root locus of the transfer function (14) coupled to a PID controller ($T_d = 0.065$, $T_f = 0.008$ and $T_i = 0.150$) with $k_p = 0.15$.

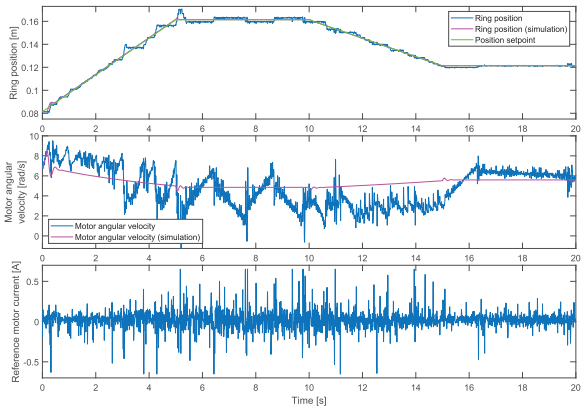

FIGURE 12. Simulation and experimental results of the control of the CRP coupled to the PID controller (17).

A specific ring position profile allowing to test the controller in different situations was chosen to evaluate its performances. The setpoint changes are implemented as linear ramps to reduce the risk of actuator saturation and illustrate tracking performance. Since the CRP is an unstable system, it must be brought close to the equilibrium point considered for the design of the controller before starting the ring position control. An initialization phase is thus implemented for the motor, consisting in bringing the system from rest to its equilibrium velocity $\bar{\omega} = 6.89$ rad/s. Fig. 12 shows the simulation and the experimental results of the CRP controlled with the PID (17).

The pink curve is almost superimposed with the green one. That illustrates the satisfying performances of the controller in simulation. On the real device, it appears that the PID controller leads to proper setpoint tracking for the ring position, without significant error. During the setpoint ramp phases, the presence of an error higher than in simulation might be explained by rod imperfections making the ring not slide homogeneously. For constant setpoint phases, the ring oscillates around its setpoint. These oscillations are explained by the integrating action of the controller coupled to friction phenomena. Indeed, as an illustration, let us consider what happened during the experiment after the first ramp overshoot occurring at $t \simeq 5$ s. At $t \simeq 5.5$ s, the ring was located slightly under its setpoint. The controller thus acted to cancel this error by increasing the motor velocity, but the ring was not able to move due to static friction. When the controller had sufficiently integrated the error, the angular velocity was then high enough that the centrifugal force overcame the gravity and the static friction, making the ring slide upwards. The ring was then located slightly higher than the setpoint and the situation was reversed, meaning now that the controller drove the motor velocity to decrease. This explains the small oscillations that are observed on the motor velocity graph for a constant reference position. It is noteworthy to mention that these oscillations could be avoided by introducing a dead zone in front of the integrating action when the reference is constant.

Even though the controller leads to proper control of the ring position, the variations of the reference current are relatively important. This causes large sudden changes in the motor angular velocity, which could damage the gearmotor over time. For this reason, a new PID was designed, assuming that the variations in the reference current come from sudden fluctuations in the position sensor signal. Lowering the value of the filter coefficient N from 8 to 5 allows filtering more the signal, hence lowering these fluctuations. Besides this, reducing the controller gain k makes it less aggressive, leading to smaller current variations. Based on the stability margins, the gain of the controller is reduced to 216 and T_i is changed from 0.15 to 0.16. Accounting for the dead times, the gain margin is 8.42 dB and the phase margin is 21.5°. The controller transfer function is

$$D_p(s) = 216\frac{(1+0.160s)}{0.160s}\frac{(1+0.065s)}{(1+0.013s)}, \tag{18}$$

and its discrete equivalent is

$$D_p(z) = \frac{1051z^2 - 2080z + 1029}{z^2 - 1.9260z + 0.9263}. \tag{19}$$

An identical experiment as in Fig. 12 has been conducted with this controller, leading to Fig. 13.

Fig. 13 shows that this less aggressive controller still allows meeting the control requirement related to the ring position. The absence of a significant overshoot can be observed due to the lower controller gain. Oscillations around the position setpoint are still present due to friction phenomena. Unlike with the initial controller, sudden velocity variations are attenuated due to smaller reference current variations.

IV. TEACHING KEY ASPECTS

In a learning framework, the CRP is an interesting didactic device aiming at illustrating several concepts of closed-loop control within a significant multidisciplinary context. The device allows visualization of control principles thanks to the rotating arm and ring displacement, which is missing in some pedagogical setups. This visual aspect is

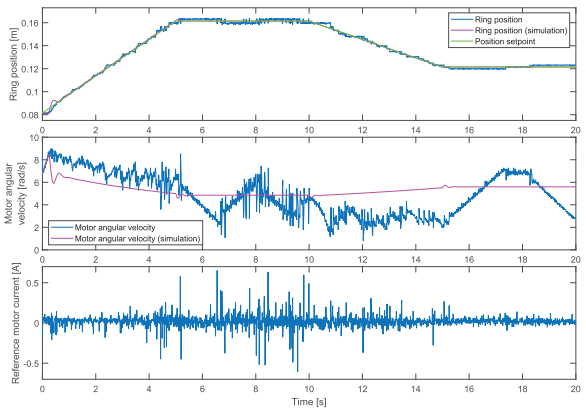

FIGURE 13. Simulation and experimental results of the control of the CRP coupled to the PID controller (19).

important since it increases the students' interest and curiosity.

From a control point of view, the CRP offers the possibility of solving control problems with different levels of complexity. Disregarding the ring, it could be used for basic control courses as a simple first-order and stable system consisting of a motor (considering the velocity control problem). Furthermore, the very same device can be used for advanced courses to control an unstable and nonlinear system through for instance the implementation of a cascade strategy. The CRP allows performing experiments such as system identification and model validation, and different controllers can be implemented (e.g., P, PD, PI, PID, state-feedback, LQG, feedforward, Lyapunov-based nonlinear control, etc.).

Furthermore, the CRP brings out some specific aspects related to the control of a real device. For example, as the ring controller is designed based on a linearized model of the system, the students have to think about a way of bringing the system close to its equilibrium point before starting the control of the ring position. In addition, the selected ring position sensor is nonlinear, thus introducing an additional challenge for students to manage. The possibility to illustrate the trade-off between closed-loop bandwidth and measurement noise rejection is also well present, as illustrated in Section III-C by the design of two different PID controllers. The treatment of noise requires instrumentation and filtering notions whereas certain mechanical knowledge is needed to properly derive the dynamic equations of the ring motion and hence obtain a precise model of the system. All these practical and multidisciplinary aspects greatly contribute to the training of the students.

The CRP presented in this paper is currently used in our department for lab sessions aiming at designing a controller which meets one or several requirements for a real plant. Other experimental setups used for similar goals in our laboratory include a heat exchanger, a rolling mill, a water tank, a house temperature simulator, a ball and beam, a ball in the tube, and a rotary inverted pendulum. Students work by teams of 3 to 4 persons and each team is associated with a plant. These labs gather students from the Université Libre de Bruxelles, Vrije Universiteit Brussels, and international students from all around the world. To increase students' experience and take benefit of the different backgrounds, the teams are created by the teaching staff in order to mix the students as much as possible. Students are given the responsibility to find the most appropriate solution to reach the control requirement of their plant. It is part of the students' work to define the effectiveness criteria of their controllers and to be able to justify the implemented solution. To achieve that goal, each team has 5 sessions of 4h laboratory sessions. These labs sessions take the form of a project where the teaching staff plays the role of questioning and coaching. Students are encouraged to work by themselves and use the knowledge from their lecture notes. This aims at increasing their critical thinking and their autonomy. These labs end up with a pooling of the work of each team through a presentation. Since each plant presents its particularities, this allows the students to share their experiences and to learn from the work of the others.

For the sake of simplicity, the Arduino initially used as microcontroller during the creation of the CRP is replaced by a National Instruments PCI-6014 acquisition board allowing the students to act on the system with the lab computer via Matlab. This facilitates the use of the CRP since students are used to work on Matlab from previous courses. In terms of programming, students do not start from scratch: they receive two Matlab codes. The first one consists of a code for model identification, allowing the estimation of a continuous-time model by solving a nonlinear least-squares problem. The second one is an example of implementation in real-time of a proportional controller.

The steps on which the students are assessed are the following:

- Determination and validation of a plant model: Students must select the most appropriate model type (black box, gray box, or white box) for their plant. This step includes the selection of an operating point. For black box identification, an example code is provided, that they have to adapt to their experiment. For physics-based model, students have to consider their operating point and use their background in classical mechanics as well as the available process characteristics for deriving a plant model and design experiments to identify the parameters. Thereafter, they must validate their candidate model by simulating it in the MATLAB/Simulink environment and comparing the simulation results with experimental data.
- Selection of an appropriate control strategy: Students must select the most effective controller given their plant and the specified control requirements.
- Design of the controllers: Based on the requirements (closed-loop system response characteristics, steady-state error, etc.), students must design an appropriate control law. They have access to computer-assisted methods from Matlab such as root locus tools and Bode

diagrams. This step also includes the selection of the sampling time, and the selection of the most appropriate control technique (for instance, in this paper we showed a control by discretization).
- Validation of the controllers in simulation: Before the implementation on the plant, students need to validate their controllers by reproducing their control scheme in Simulink.
- Validation of the controllers on the real plant: Students must modify the example code of the proportional controller to implement their controllers on the plant. This step includes the determination and the programming of the recursive equations of the controllers but also accounting for the operating point that was chosen in the modeling phase. In addition, they have to comment and critically think about the differences between simulation and reality such as noises, dead zones, and disturbances, and to come out with countermeasures if needed.

V. CONCLUSION

The objective of this paper was to present an innovative on-site pedagogical benchmark called the Centrifugal Ring Positioner (CRP) and to provide the required information to reproduce such a device. The CRP is a system consisting of a ring sliding on a rod subject to gravity and the centrifugal force induced by a motor. The design and construction of this device were carried out in a project-based learning approach consisting in assigning to a master student the development of a pedagogical device that will be used afterward by control engineering students.

By comparing the CRP with other well-known pedagogical benchmarks, remote labs, virtual labs, and take-home labs, it appears that the CRP offers interesting features. Most of its parts are 3D-printed, resulting in simple construction and architectural modifications as well as an overall relatively low cost. The total cost of the device is estimated to be less than 1000€, with the major part coming from the slip ring and the actuator (motor, motor driver, and encoder). It is easily reproducible and the design of its parts has been made available on the internet for any potentially interested user. Moreover, it presents a compact design still allowing to obtain a good illustration of control theory concepts.

Through the description of the design of the device and the selection of its electronic components, the many interconnections existing between the selection of the sensors and the actuators, the design, and the control performances were highlighted in the framework of a project-based learning approach. The contribution of this new experimental setup for the teaching of control theory within a multidisciplinary context was also pinpointed. On the one side, the CRP allows illustrating control concepts such as basic single loop and cascade control. Besides, it emphasizes several specific points originating from the implementation of a controller on a real device (trade-off between closed-loop bandwidth and noise rejection, imperfections of the components, linearization around an equilibrium point…). On the other side, classical mechanics, instrumentation, and filtering concepts are essential to reach the control specifications. All these aspects greatly contribute to the training of the students.

Although the CRP has been fully designed and properly controlled, this work has identified potential improvement areas such as:

- The design of the system, mainly of the mobile and the rod, as well as their materials could be challenged to reduce non-homogeneous friction effects.
- With small modifications, the rotating base of the CRP (motor, encoder, and slip ring) might be suitable for the design of a rotary inverted pendulum. One could therefore imagine a system with a common rotating base, being able to host either the tilted arm of the CRP or the pendulum rod of a rotary inverted pendulum. This modular design would thus lead to a twofold purpose didactic device.
- Some research work could be performed to create a take-home CRP by looking for cheaper and smaller components presenting similar dynamical and aging characteristics. This take-home version of the CRP could be preassembled and fit in a small suitcase so that the students simply have to take it out and connect the instrumentation.

REFERENCES

[1] S. D. Bencomo, "Control learning: Present and future," *IFAC Proc. Volumes*, vol. 35, no. 1, pp. 71–93, 2002. [Online]. Available: https://linkinghub.elsevier.com/retrieve/pii/S147466701540062X

[2] K. Kawlewski and P. Watroba, "Design of an inverted pendulum laboratory stand to teach mechatronics," in *Proc. 2nd Int. Conf. Chem. Process. Eng. (ICPE)*, Yogyakarta, Indonesia, 2018, Art. no. 020027. [Online]. Available: http://aip.scitation.org/doi/abs/10.1063/1.5066489

[3] J. A. Rossiter, J. Hedengren, and A. Serbezov, "Technical committee on control education: A first course in systems and control engineering," *IEEE Control Syst.*, vol. 41, no. 1, pp. 20–23, Feb. 2021.

[4] O. Boubaker, "The inverted pendulum benchmark in nonlinear control theory: A survey," *Int. J. Adv. Robot. Syst.*, vol. 10, no. 5, p. 233, May 2013. [Online]. Available: http://journals.sagepub.com/doi/10.5772/55058

[5] P. Horacek, "Laboratory experiments for control theory courses: A survey," *Annu. Rev. Control*, vol. 24, no. 1, pp. 151–162, 2000.

[6] N. Kheir, K. Åström, D. Auslander, K. Cheok, G. Franklin, M. Masten, and M. Rabins, "Control systems engineering education," *Automatica*, vol. 32, no. 2, pp. 147–166, Feb. 1996. [Online]. Available: https://linkinghub.elsevier.com/retrieve/pii/0005109896855464

[7] W. Durfee, P. Li, and D. Waletzko, "Take-home lab kits for system dynamics and controls courses," in *Proc. Amer. Control Conf.*, Boston, MA, USA, vol. 2, 2004, pp. 1319–1322. [Online]. Available: https://ieeexplore.ieee.org/document/1386757/

[8] C. M. Ionescu, E. Fabregas, S. M. Cristescu, S. Dormido, and R. De Keyser, "A remote laboratory as an innovative educational tool for practicing control engineering concepts," *IEEE Trans. Educ.*, vol. 56, no. 4, pp. 436–442, Nov. 2013. [Online]. Available: http://ieeexplore.ieee.org/document/6484200/

[9] M. A. Bochicchio and A. Longo, "Hands-on remote labs: Collaborative web laboratories as a case study for IT engineering classes," *IEEE Trans. Learn. Technol.*, vol. 2, no. 4, pp. 320–330, Oct. 2009. [Online]. Available: http://ieeexplore.ieee.org/document/5204073/

[10] C. Losada-Gutierrez, F. Espinosa, C. Santos-Perez, M. Marron-Romera, and J. M. Rodriguez-Ascariz, "Remote control of a robotic unit: A case study for control engineering formation," *IEEE Trans. Educ.*, vol. 63, no. 4, pp. 246–254, Nov. 2020. [Online]. Available: https://ieeexplore.ieee.org/document/9032350/

[11] J. Sáenz, J. Chacón, L. D. la Torre, A. Visioli, and S. Dormido, "Open and low-cost virtual and remote labs on control engineering," *IEEE Access*, vol. 3, pp. 805–814, 2015. [Online]. Available: https://ieeexplore.ieee.org/document/7119567/
[12] M. Casini, D. Prattichizzo, and A. Vicino, "A student control competition through a remote robotics lab," *IEEE Control Syst.*, vol. 25, no. 1, pp. 56–59, Feb. 2005. [Online]. Available: https://ieeexplore.ieee.org/document/1388802/
[13] M. K. Jouaneh and W. J. Palm, "Control system experiments at home," in *Proc. Frontiers Educ. Conf. (FIE)*, Rapid City, SD, USA, Oct. 2011, pp. T2G-1–T2G-6. [Online]. Available: http://ieeexplore.ieee.org/document/6143060/
[14] L. de la Torre, M. Guinaldo, R. Heradio, and S. Dormido, "The ball and beam system: A case study of virtual and remote lab enhancement with moodle," *IEEE Trans. Ind. Informat.*, vol. 11, no. 4, pp. 934–945, Aug. 2015. [Online]. Available: http://ieeexplore.ieee.org/document/7120976/
[15] C. Y. Foulis and S. Papadopoulou, "A portable low-cost arduino-based laboratory kit for control education," in *Proc. UKACC 12th Int. Conf. Control (CONTROL)*, Sheffield, U.K., Sep. 2018, p. 435. [Online]. Available: https://ieeexplore.ieee.org/document/8516817/
[16] D. Iosifidis, N. Alvanos, C. Yfoulis, S. Papadopoulou, and C. Galatsopoulos, "Practical PID hovering control of a laboratory quadcopter using low-cost embedded control hardware and software," in *Proc. UKACC 12th Int. Conf. Control (CONTROL)*, Sheffield, U.K., Sep. 2018, pp. 428–433. [Online]. Available: https://ieeexplore.ieee.org/document/8516781/
[17] R. Rutters, M. Weinheimer, and M. Bragard, "Teaching control theory with a simplified helicopter model and a classroom fitting hardware testbench," in *Proc. IEEE 59th Int. Sci. Conf. Power Electr. Eng. Riga Tech. Univ. (RTUCON)*, Riga, Latvia, Nov. 2018, pp. 1–6. [Online]. Available: https://ieeexplore.ieee.org/document/8659871/
[18] C. Gonzalez, I. Alvarado, and D. M. L. Peña, "Low cost two-wheels self-balancing robot for control education," *IFAC-PapersOnLine*, vol. 50, no. 1, pp. 9174–9179, Jul. 2017. [Online]. Available: https://linkinghub.elsevier.com/retrieve/pii/S2405896317323406
[19] A. S. Shekhawat and Y. Rohilla, "Design and control of two-wheeled self-balancing robot using Arduino," in *Proc. Int. Conf. Smart Electron. Commun. (ICOSEC)*, Trichy, India, Sep. 2020, pp. 1025–1030. [Online]. Available: https://ieeexplore.ieee.org/document/9215421/
[20] C. Xu, M. Li, and F. Pan, "The system design and LQR control of a two-wheels self-balancing mobile robot," in *Proc. Int. Conf. Electr. Control Eng.*, Yichang, China, Sep. 2011, pp. 2786–2789. [Online]. Available: http://ieeexplore.ieee.org/document/6057680/
[21] R. S. Barbosa, "Educational platform for modeling and control," in *Proc. 14th Technol. Appl. Electron. Teach. Conf. (TAEE)*, Porto, Portugal, Jul. 2020, pp. 1–9. [Online]. Available: https://ieeexplore.ieee.org/document/9163746/
[22] J. Pereira and J. Bowles, "Comparing controllers with the ball in a tube experiment," in *Proc. IEEE 5th Int. Fuzzy Syst.*, New Orleans, LA, USA, vol. 1, Sep. 1996, pp. 504–510. [Online]. Available: http://ieeexplore.ieee.org/document/551792/
[23] D. E. Seborg, T. F. Edgar, D. A. Mellichamp, and F. J. Doyle, III, "Enhanced single-loop control strategies," in *Process Dynamics and Control*, 3rd ed. Hoboken, NJ, USA: Wiley, 2011, pp. 289–294.
[24] S.-K. Oh, H.-J. Jang, and W. Pedrycz, "Optimized fuzzy PD cascade controller: A comparative analysis and design," *Simul. Model. Pract. Theory*, vol. 19, no. 1, pp. 181–195, Jan. 2011. [Online]. Available: https://linkinghub.elsevier.com/retrieve/pii/S1569190X10001255

XAVIER JORDENS was born in Anderlecht, Belgium, in 1997. He received the B.S. and M.S. degrees in chemical engineering from the Université Libre de Bruxelles (ULB), Belgium, in 2018 and 2020, respectively.

He is currently a Teaching Assistant with the Department of Control Engineering and System Analysis, ULB. His research interests include control engineering, development of control teaching labs, constrained control, and autonomous navigation of marine vehicles.

ROBIN WILMART was born in Montigny-le-Tilleul, Belgium, in 1990. He received the B.S. and M.S. degrees in mechanical engineering specializing in automation from the University of Mons, Belgium, in 2011 and 2013, respectively.

From 2013 to 2015, he worked in the telecommunication industry. Since 2016, he has been a Teaching Assistant with the Department of Control Engineering and System Analysis, Université Libre de Bruxelles, Belgium. His research interest includes the development and design of a six degrees of freedom goniometer allowing consistent measurements of the knee kinematics.

EMANUELE GARONE (Member, IEEE) received the Ph.D. degree in systems engineering from the University of Calabria, Italy, in 2009.

Since 2010, he has been an Associate Professor with the Control Design and System Analysis Department, Université Libre de Bruxelles, Brussels, Belgium. He has authored approximately 150 papers in international journals and peer-reviewed conferences. His main research interests include the control of systems subject to constraints with a particular focus on the reference governor framework and the development of constrained control strategy with a low computational footprint. In recent years, he has introduced the original concept of Explicit Reference Governor that allows the control of systems subject to constraints without the use of any online optimization. He is also very active in the application of constrained control strategies to mechatronics and aerial systems. His other research interests include nonlinear control, distributed and networked control systems, precision agriculture, and aerial robotics.

MICHEL KINNAERT (Member, IEEE) graduated in mechanical and electrical engineering from the Université Libre de Bruxelles (ULB), Brussels, Belgium, in 1983. He received the M.S. degree in electrical engineering from Stanford University, in 1984, and the Ph.D. degree from ULB, in 1987.

After being employed for six years by the Belgian National Fund for Scientific Research, he was appointed by ULB where he is currently a Full Professor with the Department of Control Engineering and System Analysis. He held visiting professor positions at Université Claude Bernard Lyon I, Lyon, France. He has coauthored, with M. Blanke, J. Lunze, and M. Staroswiecki, the book *Diagnosis and Fault-Tolerant Control* (Second Edition, Springer, 2006). His research interests include fault detection and isolation, and fault tolerant control, with applications in energy storage and production as well as mechatronics. He was the Chairperson of the IFAC Technical Committee SAFEPROCESS from 2002 to 2008. He has been an Associate Editor of the *Control Engineering Practice* (IFAC) since 2005.

LAURENT CATOIRE received the master's degree in electromechanical engineering from the Université Libre de Bruxelles (ULB), Belgium, in 1997.

Since 1997, he has been a member of the Department of Control Engineering and System Analysis, ULB. Since 2016, he has also held the position of the Technical Director at the Ecole Polytechnique de Bruxelles. His research interests mainly include the design and the control of pilot-scale processes for teaching and research purposes, the monitoring and control of processes, and project-based learning.